https://doi.org/10.5194/hess-2020-572
Preprint. Discussion started: 23 November 2020

Hydrology and Earth System Sciences
Open Access
Discussions

Technical note: Discharge response of a confined aquifer with variable thickness to temporal nonstationary random recharge processes

Ching-Min Chang[1], Chuen-Fa Ni[1], We-Ci Li[1], Chi-Ping Lin[2], and I-Hsian Lee[2]

[1]Graduate Institute of Applied Geology, National Central University, Taoyuan, Taiwan

[2]Center for Environmental Studies, National Central University, Taoyuan, Taiwan

Correspondence: Chuen-Fa Ni (nichuenfa@geo.ncu.edu.tw)

https://doi.org/10.5194/hess-2020-572
Preprint. Discussion started: 23 November 2020

Hydrology and Earth System Sciences
Discussions

Abstract. This work develop a transfer function to describe the variation of the integrated specific discharge in response to the temporal variation of the rainfall event in the frequency domain. It is assumed that the rainfall-discharge process takes place in a confined aquifer with variable thickness, and it is treated as nonstationary in time to represent the stochastic nature of the hydrological process. The presented transfer function can be used to quantify the variability of the integrated discharge field induced by the variation of rainfall field or to simulate the discharge response of the system to any varying rainfall input at any time resolution using the convolution model. It is shown that with the Fourier-Stieltjes representation approach a closed-form expression for the transfer function in the frequency domain can be obtained, which provide a basis for the analysis of the influence of controlling parameters occurring in the rainfall rate and integrated discharge models on the transfer function.

1 Introduction

Quantifying the variability of specific discharge response of an aquifer system to fluctuations in inflow recharge is essential for efficient groundwater resources management. However, this requires extensive and continuous hydrological time-series data, and these data are very often not available in practice. One possible

https://doi.org/10.5194/hess-2020-572
Preprint. Discussion started: 23 November 2020

Hydrology and Earth System Sciences
Discussions

approach (namely, convolution or transfer function approach) to this problem is to simulate the discharge response by convolution of the time-varying recharge input with the corresponding impulse response. In convolution models, the aquifer is regarded as a filter that converts recharge signals into fluctuations of the aquifer head or discharge. Lumped conceptual-convolution models have been shown to be an efficient means for the simulation of time series of groundwater levels (e.g., Gelhar, 1974; Molénat et al., 1999; Olsthoorn, 2007; Long and Mahler, 2013; Pedretti et al., 2016).

Since the impulse response function in the convolution model contains all information of the system necessary to relate its input to its output, it may be determined from the analytical solution of the linear system equation governing the input-output process (e.g., Cooper and Rorabaugh, 1963). Once a suitable impulse response function can be specified, it allows the simulation of the linear system response to any varying input at any time resolution.

In this work, a regional-scale flow in a confined aquifer with variable thickness, which is recharged by rainfall through an outcrop, is analyzed by deriving transfer functions to characterize the rainfall-discharge process in the frequency domain. The stochastic analysis of groundwater flow is traditionally based on the assumption of stationarity of the recharge and discharge processes. However, the hydrologic process

https://doi.org/10.5194/hess-2020-572
Preprint. Discussion started: 23 November 2020

Hydrology and Earth System Sciences
Discussions

in nature is nonstationary-stochastic (e.g., Christensen and Lettenmaier, 2007; Milly et al., 2008; Sang et al., 2018). In order to improve the quantification of the natural recharge-discharge process, the nonstationary rainfall-discharge process is assumed in this study. The Fourier-Stieltjes representation approach is used to achieve the goal of this work. The analysis of the results is focused on the influence of controlling parameters in the rainfall-discharge models on the transfer function.

2 Problem formulation

This study regards the entire confined aquifer of variable thickness with stochastic rainfall recharge and thus stochastic outflow as a single lumped linear system. This means that the control volume is extended to the scale of an aquifer, so that the flow variables are integrated in space and only the temporal variability is preserved. In this way, the output of the system can be represented as a linear combination of the responses to each of the basic inputs (e.g., Rugh, 1981; Rinaldo & Marani, 1987)

$$Q(t) = \int_0^t \varphi(t,\tau) R(\tau) d\tau \,, \tag{1}$$

where Q and R denote the output flow rate and the input flow (or recharge) rate of the system, respectively, and φ is the impulse response function of the system. This implies that once an appropriate impulse response function can be specified on the

https://doi.org/10.5194/hess-2020-572
Preprint. Discussion started: 23 November 2020

aquifer scale, the evaluation of the system response does not require the specification of a smaller scale heterogeneity.

When using the nonstationary Fourier-Stieltjes representations for the perturbed quantities of random recharge and outflow discharge processes, namely (e.g., Priestley, 1965)

$$r(t) = R(t) - E[R(t)] = \int_{-\infty}^{\infty} \Lambda_r(t;\omega) dZ_\xi(\omega)\,, \tag{2}$$

$$q(t) = Q(t) - E[Q(t)] = \int_{-\infty}^{\infty} \Lambda_q(t;\omega) dZ_\xi(\omega)\,, \tag{3}$$

the power spectrum of the mean-removed convolution (1) can be written in the form

$$S_{qq}(t;\omega) = \left|\Lambda_q(t:\omega)\right|^2 S_{\xi\xi}(\omega)\,, \tag{4}$$

where

$$\Lambda_q(t;\omega) = \int_0^t \varphi(t,\tau)\Lambda_r(\tau;\omega) d\tau\,. \tag{5}$$

In Eqs. (2) and (3), Λ_r and Λ_q are the oscillatory functions (Priestley, 1965) of the recharge and outflow processes, respectively, ω is the frequency, ξ is a zero-mean random stationary forcing process, which generates the variations of the recharge and thus the output flow processes, with an orthogonal increment dZ_ξ. In Eq. (4), S_{qq} and $S_{\xi\xi}$ represent the power spectra of the processes q and ξ, respectively, and $|\Lambda_q|^2$ is termed the transfer function.

In practice, the interest in many cases resides in evaluating the influence of the

https://doi.org/10.5194/hess-2020-572
Preprint. Discussion started: 23 November 2020

variation of recharge on the variation of the outflow discharge. Equation (4) provides an efficient way to quantify the variability of the outflow induced by the fluctuations of the inflow process in the frequency domain, since it relates the fluctuations of an output time series to those of an input series.

It is worthwhile to mention that for the case of second-order stationary rainfall processes, the representations of the forms (2) and (3) are reduced, respectively, to

$$r(t) = \int_{-\infty}^{\infty} e^{i\omega t} dZ_r(\omega) , \tag{6}$$

$$q(t) = \int_{-\infty}^{\infty} \Lambda_q(t;\omega) dZ_r(\omega) , \tag{7}$$

and correspondingly

$$S_{qq}(t;\omega) = \left|\Lambda_q(t:\omega)\right|^2 S_{rr}(\omega) , \tag{8}$$

where

$$\Lambda_q(t;\omega) = \int_{0}^{t} \varphi(t,\tau) e^{i\omega t} d\tau . \tag{9}$$

Equations (1) and (4) reveal that once the transfer function for the linear lumped system is identified, the first two moments of temporal random discharge fields can be determined. That is, the transfer function approach provides a basic framework for the characterization of large-scale flow processes, which may service as a basis for an efficient management of groundwater resources. Furthermore, Eq. (4) provides another possible way to identify the aquifer parameters, as it relates the observed

https://doi.org/10.5194/hess-2020-572
Preprint. Discussion started: 23 November 2020

Hydrology and Earth System Sciences
Discussions

fluctuations of an output discharge process to those of a recharge process in the frequency domain.

In the following, the focus is on the development of a closed-form expression for the transfer function for a linear lumped confined flow model, in which the regional confined aquifer is directly recharged by rainfall in the area corresponding to the high elevation outcrop.

3 Theoretical development

The differential equation describing the transient flow of groundwater in inhomogeneous isotropic confined aquifers is of the form (e.g., Bear, 1979; de Marsily, 1986)

$$S_s \frac{\partial}{\partial t} h(\boldsymbol{x},t) = \frac{\partial}{\partial x_i}[K(\boldsymbol{x}) \frac{\partial}{\partial x_i} h(\boldsymbol{x},t)] \qquad i = 1, 2, 3, \tag{10}$$

in which S_s represents the specific storage coefficient of the aquifer, $h = h(\boldsymbol{x},t)$ is the hydraulic head, $K(\boldsymbol{x})$ is the hydraulic conductivity, and $\boldsymbol{x}$ (= (x_1,x_2,x_3)) is the spatial coordinate vector. Many problems of groundwater flow are regional in nature, with the horizontal extent of the formation being much larger than the vertical extent. It is more practical to regard the flow as essentially horizontal. The regional-scale flow equations can be derived by integrating Eq. (10) along the thickness of the confined

https://doi.org/10.5194/hess-2020-572
Preprint. Discussion started: 23 November 2020

Hydrology and Earth System Sciences
Discussions

aquifer using the assumption of vertical equipotential surfaces (e.g., Bear, 1979; Bear and Cheng, 2010).

Integrating Eq. (10) along the x_3-axis perpendicular to the confining beds and using Leibnitz' rule results in

$$S(x_1,x_2)\frac{\partial}{\partial x_i}\tilde{h}(x_1,x_2,t)=\frac{\partial}{\partial x_i}\left[T(x_1,x_2)\frac{\partial}{\partial x_i}\tilde{h}(x_1,x_2,t)\right]+T(x_1,x_2)\frac{\partial}{\partial x_i}\ln B(x_1,x_2)\frac{\partial}{\partial x_i}\tilde{h}(x_1,x_2,t), \quad i=1,2 \quad (11)$$

where $S(x_1,x_2)$ is the storage coefficient (or storativity) of the aquifer (= $S_sB(x_1,x_2)$), $B(x_1,x_2) = b_2(x_1,x_2)$-$b_1(x_1,x_2)$ (an aquifer's thickness), $T(x_1,x_2)$ is the transmissivity of the aquifer (=$K(x_1,x_2)B(x_1,x_2)$), interpreted as the depth-integrated hydraulic conductivity, and $\tilde{h}(x_1,x_2,t)$ is the depth-averaged hydraulic head defined as

$$\tilde{h}(x_1,x_2)=\frac{1}{b_2(x_1,x_2)-b_1(x_1,x_2)}\int_{b_1(x_1,x_2)}^{b_2(x_1,x_2)} h(x_1,x_2,x_3,t)dx_3, \quad (12)$$

Equation (11) is derived under the following assumptions: (1) there is no exchange of leakage fluxes between the confined aquifer and its confining beds in the direction of x_3-axis, and (2) $h(x_1,x_2,b_2,t) \approx \tilde{h}(x_1,x_2,t) \approx h(x_1,x_2,b_1,t)$ (vertical equipotentials; Bear, 1979; Bear and Cheng, 2010). Similarly, when applying Leibnitz' rule to Darcy equation, the vertically integrated specific discharge in the x_i direction is given by

$$Q_{x_i}(x_1,x_2,t)=-K(x_1,x_2)B(x_1,x_2)\frac{\partial}{\partial x_i}\tilde{h}(x_1,x_2,t)=-T(x_1,x_2)\frac{\partial}{\partial x_i}\tilde{h}(x_1,x_2,t). \quad i=1,2 \quad (13)$$

If the regional confined aquifer has nonuniform, unidirectional mean flow in the direction of x_1-axis, but with small flow fluctuations in the direction of x_1- and x_2-axis and time-varying recharge at the aquifer outcrop (x_1 = 0), the groundwater flow may

https://doi.org/10.5194/hess-2020-572
Preprint. Discussion started: 23 November 2020

Hydrology and Earth System Sciences
Open Access
Discussions

be regarded as one-dimensional, so that Eqs. (11) and (13) can be approximated, respectively, by

$$\frac{S(x)}{\overline{T}}\frac{\partial}{\partial t}\tilde{h}(x,t)=\frac{\partial^2}{\partial x^2}\tilde{h}(x,t)+\frac{\partial}{\partial x}\ln\overline{T}(x)\frac{\partial}{\partial x}\tilde{h}(x,t)+\frac{\partial}{\partial x}\ln B(x)\frac{\partial}{\partial x}\tilde{h}(x,t)+\frac{R(t)}{\overline{T}}, \tag{14}$$

$$Q_x(x,t)=-\overline{T}(x)\frac{\partial}{\partial x}\tilde{h}(x,t), \tag{15}$$

where $\overline{T}$ = $\overline{K}B$, $\overline{K}$ represents the spatial average of the hydraulic conductivity, and R is the recharge rate. Equation (14) can be expressed alternatively as

$$\frac{S_s}{\overline{K}}\frac{\partial}{\partial t}\tilde{h}(x,t)=\frac{\partial^2}{\partial x^2}\tilde{h}(x,t)+2\frac{\partial}{\partial x}\ln B(x)\frac{\partial}{\partial x}\tilde{h}(x,t)+\frac{R(t)}{\overline{K}B(x)}. \tag{16}$$

for the convenient analysis of the effect of the thickness of the aquifer.

In the following analysis, the recharge rate is considered a random function of time. Equation (15) is then regarded as a stochastic differential equation with a stochastic input in time and therefore a stochastic output in time. Introduction of decomposition of the depth-averaged hydraulic head into a mean and a zero-mean perturbation into Eq. (16) and, after subtracting the mean of the resulting equation from Eq. (16), the result is the following equation describing the depth-averaged head perturbation

$$\frac{S_s}{\overline{K}}\frac{\partial}{\partial t}h'(x,t)=\frac{\partial^2}{\partial x^2}h'(x,t)+2\frac{\partial}{\partial x}\ln B(x)\frac{\partial}{\partial x}h'(x,t)+\frac{r(t)}{B(x)\overline{K}}, \tag{17}$$

where h'(x,t) is the fluctuations in depth-averaged head.

If it is assumed that the thickness of confined aquifer increase in x-direction in accordance with (Hantush, 1962; Marino and Luthin, 1982)

https://doi.org/10.5194/hess-2020-572
Preprint. Discussion started: 23 November 2020

$$B(x) = \beta e^{\alpha x}, \tag{18}$$

then Eq. (17) becomes

$$\frac{S_s}{\overline{K}} \frac{\partial}{\partial t} h'(x,t) = \frac{\partial^2}{\partial x^2} h'(x,t) + 2\alpha \frac{\partial}{\partial x} h'(x,t) + \frac{e^{-\alpha x}}{\beta \overline{K}} r(t). \tag{19}$$

In Eq. (18), β and α are positive geometrical parameters. Furthermore, the outcrop (x = 0) and outlet (x = L) of the confined aquifer are considered as constant head boundaries. Since Eq. (19) only quantifies the response of the depth-averaged head to changes in the recharge rate, the initial and boundary conditions for Eq. (19) may be represented as follows

$$h'(x,0;\omega) = 0, \tag{20a}$$

$$h'(0,t;\omega) = 0, \tag{20b}$$

$$h'(L,t;\omega) = 0. \tag{20c}$$

The following Fourier-Stieltjes integral representation of a depth-averaged head process is used to solve Eqs. (19) and (20) for the fluctuations h' in terms of r:

$$h'(x,t) = \int_{-\infty}^{\infty} \Lambda_h(t;\omega) dZ_{\xi}(\omega), \tag{21}$$

where Λ_h is the oscillatory function of depth-averaged head process. The resulting differential equation for the oscillatory functions is found from using Eqs. (2) and (21) in Eqs. (19) and (20) as

$$\frac{S_s}{\overline{K}} \frac{\partial}{\partial t} \Lambda_h(x,t;\omega) = \frac{\partial^2}{\partial x^2} \Lambda_h(x,t;\omega) + 2\alpha \frac{\partial}{\partial x} \Lambda_h(x,t;\omega) + \frac{e^{-\alpha x}}{\beta \overline{K}} \Lambda_r(t;\omega). \tag{22}$$

with the following conditions:

https://doi.org/10.5194/hess-2020-572
Preprint. Discussion started: 23 November 2020

$$\Lambda_h(x,0;\omega)=0\,, \tag{23a}$$

$$\Lambda_h(0,t;\omega)=0\,, \tag{23b}$$

$$\Lambda_h(L,t;\omega)=0\,. \tag{23c}$$

By solving the above boundary value problem, the oscillatory function of depth-averaged head process is found to be (see Appendix A)

$$\Lambda_h(x,t;\omega)=\frac{2}{S_s\beta}\sum_{n=1}^{n=\infty}\frac{1-\cos(n\pi)}{n\pi}\exp(-\mu\frac{x}{L})\sin(n\pi\frac{x}{L})\int_0^t\exp[-\theta_n(t-\tau)]\Lambda_r(\tau;\omega)d\tau\,, \tag{24}$$

where $\mu=\alpha L$ and $\theta_n=\overline{K}(n^2\pi^2+\mu^2)/(S_sL^2)$. It implies from Eqs. (3), (15) and (24) that at the arbitrary location $x=x_\varepsilon$,

$$\Lambda_q(t;\omega)=\Lambda_{q_x}(x_\varepsilon,t;\omega)$$

$$=-2\frac{\overline{K}}{S_sL}\sum_{n=1}^{n=\infty}\frac{1-\cos(n\pi)}{n\pi}[n\pi\cos(n\pi\Upsilon)-\mu\sin(n\pi\Upsilon)]\int_0^t\exp[-\theta_n(t-\tau)]\Lambda_r(\tau;\omega)d\tau\,, \tag{25}$$

where $\Upsilon=x_\varepsilon/L$. This means that the impulse response function of the system φ in Eqs. (1) or (5) is taken in the form

$$\varphi(t,\tau)=-2\frac{\overline{K}}{S_sL}\sum_{n=1}^{n=\infty}\frac{1-\cos(n\pi)}{n\pi}[\cos(n\pi\Upsilon)-\mu\sin(n\pi\Upsilon)]\exp[-\theta_n(t-\tau)]\,. \tag{26}$$

4 Results and discussion

Equation (25) implies that the transfer function $|\Lambda_q|^2$ depends on the oscillatory function of the temporal random rainfall process; consequently, to complete the analysis of the transfer function the oscillatory function of the temporal random rainfall process must be specified. It is assumed that the generated temporal random perturbations of rainfall field are governed by the noise forced diffusive rainfall model (North et al., 1993)

$$\tau_0 \frac{\partial}{\partial t}\rho(x,t) = \lambda_0^2 \frac{\partial^2}{\partial x^2}\rho(x,t) - \rho(x,t) + \xi(t)\,, \tag{27}$$

where ρ is a zero-mean rainfall rate perturbation, τ_0 and λ_0 are the characteristic time and length scales, respectively, which are inherent to the rainfall field, and ξ is a zero-mean random stationary forcing process which has a spectral representation of the form (e.g., Lumley and Panofsky, 1964)

$$\xi(t) = \int_{-\infty}^{\infty} e^{i\omega t} dZ_{\xi}(\omega)\,. \tag{28}$$

In Eq. (27), the rainfall-rate field is represented as a first-order continuous autoregressive process in time and an isotropic second-order autoregressive process in space.

Furthermore, the rest of this study takes into account that rain falls within a defined period of time over a certain area of horizontal extension from $x = -\ell$ to $x = \ell$. As such, the initial and boundary conditions for rainfall rate perturbations may be represented by

$$\rho(x,0) = 0\,, \tag{29a}$$

$$\rho(-\ell,t) = 0\,, \tag{29b}$$

https://doi.org/10.5194/hess-2020-572
Preprint. Discussion started: 23 November 2020

Hydrology and Earth System Sciences
Open Access
EGU
Discussions

$$\rho(\ell,t)=0\,. \tag{29c}$$

4.1 Nonstationary random rainfall fields in time

Using the Fourier-Stieltjes integral representation for the perturbation ρ,

$$\rho(x,t)=\int_{-\infty}^{\infty}\Lambda_{\rho}(t;\omega)dZ_{\xi}(\omega)\,, \tag{30}$$

and Eq. (28) in Eq. (27), it follows that

$$\tau_0\frac{\partial}{\partial t}\Lambda_{\rho}(x,t;\omega)=\lambda_0^2\frac{\partial^2}{\partial x^2}\Lambda_{\rho}(x,t;\omega)-\Lambda_{\rho}(x,t;\omega)+e^{i\omega t}\,, \tag{31}$$

where Λ_{ρ} is the oscillatory function of the rainfall rate processes. With the application of the initial and boundary conditions,

$$\Lambda_{\rho}(x,0;\omega)=0\,, \tag{32a}$$

$$\Lambda_{\rho}(-\ell,t;\omega)=0\,, \tag{32b}$$

$$\Lambda_{\rho}(\ell,t;\omega)=0\,, \tag{32c}$$

the solution of Eqs. (31) and (32) is given by (see Appendix B)

$$\Lambda_{\rho}(x,t;\omega)=2\sum_{m=1}^{m=\infty}\frac{1-\cos(m\pi)}{m\pi}\sin(m\pi\frac{x+\ell}{2\ell})\frac{\exp(i\Omega_t)-\exp(-\Theta_m t/\tau_0)}{\Theta_m+i\Gamma}\,, \tag{33}$$

where Θ_m = $1+m^2\pi^2\eta^2$, $\eta=\lambda_0/(2\,\ell\,)$, $\Omega_t=\omega t$, and $\Gamma=\omega\tau_0$.

In the case where the regional confined aquifer is directly recharged by rainfall at the aquifer outcrop (x = 0), the oscillatory function is reduced to

$$\Lambda_r(t;\omega)=\Lambda_\rho(0,t;\omega)=2\sum_{m=1}^{m=\infty}\frac{1-\cos(m\pi)}{m\pi}\sin(m\frac{\pi}{2})\frac{\exp(i\Omega_t)-\exp(-\Theta_m t/\tau_0)}{\Theta_m+i\Gamma}\,. \quad (34)$$

Correspondingly, the power spectrum of rainfall rate, $S_{rr}(t,\omega)$, can be expressed by

$$S_{rr}(t;\omega)=\left|\Lambda_r(t;\omega)\right|^2 S_{\xi\xi}(\omega)$$

$$=4\sum_{n=1}^{n=\infty}\sum_{m=1}^{m=\infty}\frac{1-\cos(m\pi)}{m\pi}\frac{1-\cos(n\pi)}{n\pi}\sin(m\frac{\pi}{2})\sin(n\frac{\pi}{2})\frac{1}{\Theta_m^2+\Gamma^2}\frac{1}{\Theta_n^2+\Gamma^2}$$

$$\left\{(\Theta_m\Theta_n+\Gamma^2)[1+T_1-T_2\cos(\Omega_t)]-T_3\Gamma(\Theta_m-\Theta_n)\sin(\Omega_t)\right\}S_{\xi\xi}(\omega)\,, \quad (35)$$

where $T_1=\exp[-(\Theta_m+\Theta_n)t/\tau_0]$, $T_2=\exp(-\Theta_m t/\tau_0)+\exp(-\Theta_n t/\tau_0)$, and $T_3=\exp(-\Theta_m t/\tau_0)-\exp(-\Theta_n t/\tau_0)$.

The transfer function of the rainfall processes in Eq. (35) behaves like a filter, attenuating the high-frequency part of the rainfall spectrum. The graph of transfer function, which is characterized by the characteristic time scale τ_0 for different characteristic length scales, is shown in Fig. 1. It clearly shows a reduction of the transfer function with increasing τ_0, implying a reduction of the variability of the rainfall field with the characteristic time scale of the rainfall field. A larger τ_0 decreases the temporal persistence of the rainfall fluctuations, resulting in a smaller transfer function. It is also seen that for a fixed value of the time scale, the transfer function of the rainfall processes tends to decrease as the length scale of the rainfall field increases. The influence of the length scale plays a similar role as the influence of the time scale in reducing the temporal persistence of the rainfall fluctuations and thus the variability of the rainfall field.

https://doi.org/10.5194/hess-2020-572
Preprint. Discussion started: 23 November 2020

Hydrology and Earth System Sciences
Open Access
Discussions

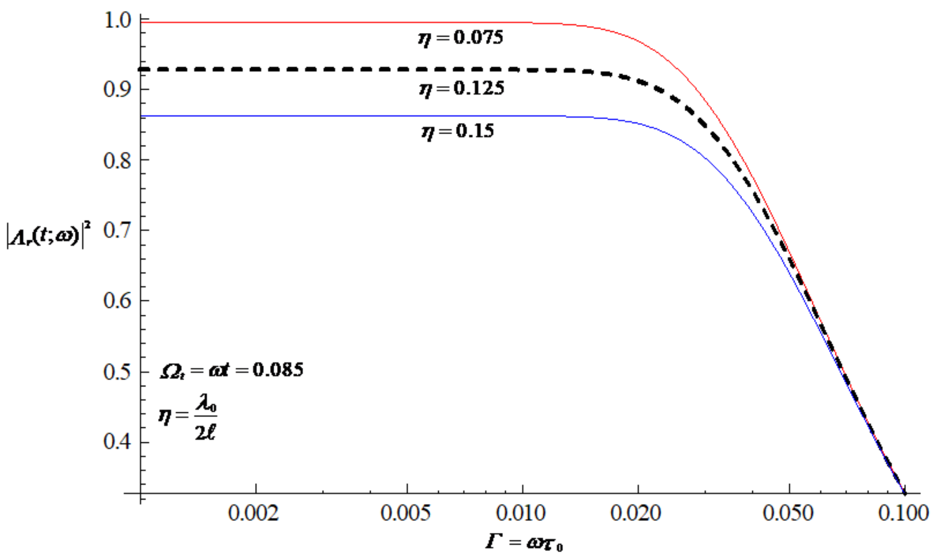

Figure 1. Graphical representation of the transfer function of the rainfall processes in Eq. (35) characterized by the time scale for different length scales, where the series calculation is truncated up to $M = N = 100$.

Through the use of Eq. (25) and Eq. (34), the oscillatory function of the integrated discharge process could be represented as follows:

$$\Lambda_q(t;\omega) = -4\frac{\overline{K}}{S_s L}\sum_{n=1}^{n=\infty}\frac{1-\cos(n\pi)}{n\pi}[n\pi\cos(n\pi\Upsilon)-\mu\sin(n\pi\Upsilon)]$$

$$\times\sum_{m=1}^{m=\infty}\frac{1-\cos(m\pi)}{m\pi}\frac{\sin(m\frac{\pi}{2})}{\Theta_m+i\Gamma}\left[\frac{\exp(i\Omega_t)-\exp(-\theta_n t)}{\theta_n+i\omega}-\frac{\exp(-\Theta_m t/\tau_0)-\exp(-\theta_n t)}{\theta_n-\Theta_m/\tau_0}\right] . \quad (36)$$

Thus, the transfer function of the integrated discharge flux is taken in the form

https://doi.org/10.5194/hess-2020-572
Preprint. Discussion started: 23 November 2020

$$\frac{S_{qq}(t;\omega)}{S_{\xi\xi}(\omega)} = \left|\Lambda_q(t;\omega)\right|^2 = 16L^2\vartheta^2\left\{\left[\sum_{n=1}^{n=\infty}\sum_{m=1}^{m=\infty}\Psi_1\Psi_2\left(\frac{\Theta_m\Psi_3+\Gamma\Psi_4}{\theta_n^2\tau_0^2+\Gamma^2}+\frac{\Theta_m\Psi_5}{\Theta_m-\theta_n\tau_0}\right)\right]^2\right.$$

$$\left.+\left[\sum_{n=1}^{n=\infty}\sum_{m=1}^{m=\infty}\Psi_1\Psi_2\left(\frac{\Theta_m\Psi_4-\Gamma\Psi_3}{\theta_n^2\tau_0^2+\Gamma^2}-\frac{\Gamma\Psi_5}{\Theta_m-\theta_n\tau_0}\right)\right]^2\right\}, \tag{37}$$

where $\vartheta = \overline{K}\,\tau_0/(S_s L^2)$ and

$$\Psi_1 = \frac{1}{\Theta_m^2+\Gamma^2}\frac{1-\cos(m\pi)}{m\pi}\sin(m\frac{\pi}{2}), \tag{38a}$$

$$\Psi_2 = \frac{1-\cos(n\pi)}{n\pi}[\cos(n\pi\Upsilon)-\mu\sin(n\pi\Upsilon)], \tag{38b}$$

$$\Psi_3 = \Gamma\sin(\Omega_t)+\theta_n\tau_0[\cos(\Omega_t)-\exp(-\theta_n t)], \tag{38c}$$

$$\Psi_4 = \theta_n\tau_0\sin(\Omega_t)-\Gamma[\cos(\Omega_t)-\exp(-\theta_n t)], \tag{38d}$$

$$\Psi_5 = \exp(-\Theta_m t/\tau_0)-\exp(-\theta_n t)\,. \tag{38e}$$

An essential feature of the transfer function of the integrated discharge flux in Eq. (37) is the resulting filtering associated with the flow process, as shown in Fig. 2. The attenuating the high-frequency part of the flow discharge spectrum means that the flow process smooths-out much of the small-scale variations caused by the rainfall field. Physically, this feature implies that the flow field is much smoother than the rainfall field. The figure also shows that the transfer function at fixed values for frequency and time increases with the increasing thickness of the confined aquifer. An increase in the thickness of the aquifer leads to an increased temporal persistence of the flow discharge fluctuations caused by the variation of the rainfall field and thus to an increase in the variability of integrated discharge field. As shown in Fig. 3, the ratio of the mean hydraulic conductivity to the storage coefficient (often referred to as

https://doi.org/10.5194/hess-2020-572
Preprint. Discussion started: 23 November 2020

Hydrology and Earth System Sciences
Open Access
Discussions

the aquifer diffusivity) plays a similar role in influencing the variation of the transfer function as the thickness of the confined aquifer. The introduction of a larger aquifer diffusivity leads to a larger transfer function of integrated discharge and thus to a larger variability of the discharge field. Since the variability of the discharge field is positively correlated with that of rainfall field, the variability of the integrated discharge field will decrease with increasing characteristic time or length scale of the rainfall field (see Fig. 1).

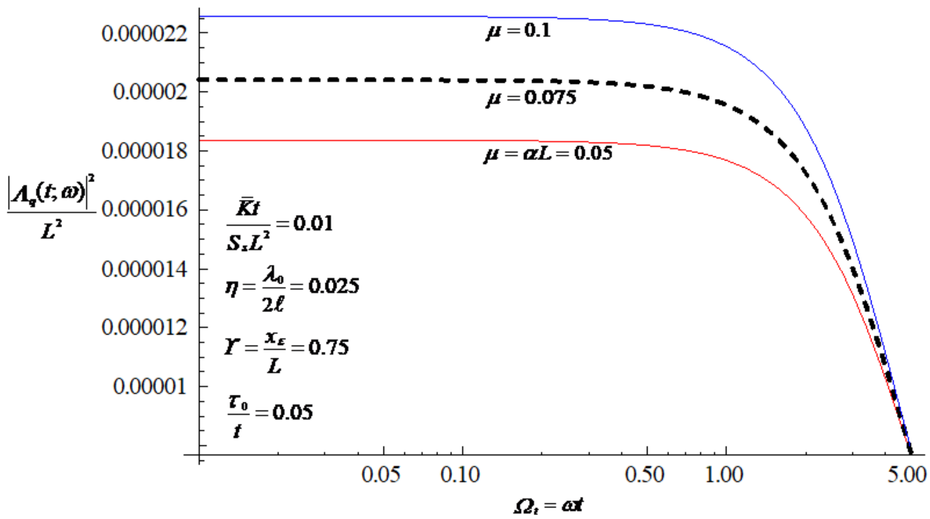

Figure 2. Influence of the thickness of the confined aquifer on the transfer function of the discharge flux, where the series calculation is truncated up to $M = N = 100$.

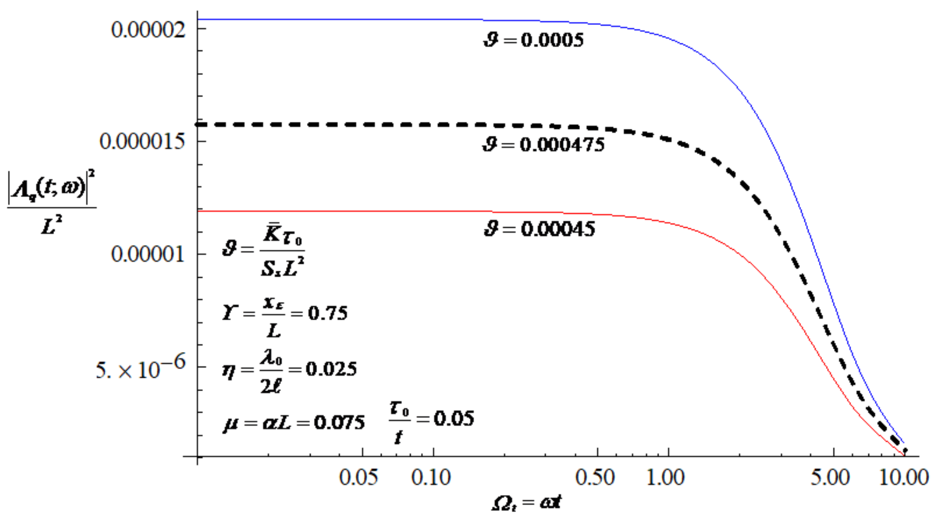

Figure 3. Influence of the aquifer diffusivity on the transfer function of the discharge flux, where the series calculation is truncated up to $M = N = 100$.

From Eqs. (4) or (8), the transfer function can be defined as the ratio of the fluctuations of an observation of output time series to those of input time series in frequency domain. Equations (35) and (37) indicate that the transfer functions are related to the properties of the rainfall field and the aquifer, such as the characteristic scales of time and length of rainfall field and the diffusivity and thickness parameters of the aquifer. Therefore, the transfer function derived here has the potential to perform a parameter estimation based on the observations of input and output time series using the inverse modeling approach.

Good modeling practice requires an assessment of the uncertainties associated

https://doi.org/10.5194/hess-2020-572
Preprint. Discussion started: 23 November 2020

Hydrology and Earth System Sciences
Discussions

with the model predictions. The variance can be treated as a quantitative measure of the uncertainty. A result such as the integration of Eq. (37) over the frequency domain for a given spectrum of observed inflow variations could serve as a calibration target when applying the mean value model to field situations. The mean discharge can be determined from the mean value of Eq. (1) with the impulse response function defined by Eq. (26).

Climate changes have a direct influence on the rainfall event (e.g., Trenberth, 2011; Pendergrass et al., 2014; Eekhout et al., 2018). The nonstationarity in the statistical properties of rainfall field is a representation of climate change (e.g., Razavi et al., 2015; López and Francés, 2013; Benoit et al., 2020). The effect of climatic change on variability of groundwater specific discharge has not yet been well characterized in the literature. The transfer function in Eq. (37), which relates the nonstationary spectra of the rainfall fluctuations to those of integrated discharge variation, has the potential to analyze the effects of climate change on groundwater specific discharge variability.

4.2 A note on stationary random rainfall fields in time

If the temporal random rainfall fields are stationary, there exists a representation of

https://doi.org/10.5194/hess-2020-572
Preprint. Discussion started: 23 November 2020

Hydrology and Earth System Sciences
Discussions

the rainfall perturbation process in terms of a Fourier-Stieltjes integral as Eq. (6). Substituting Eqs. (6) and (21) into Eq. (19) gives

$$\frac{S_s}{\overline{K}}\frac{\partial}{\partial t}\Lambda_h(x,t;\omega)=\frac{\partial^2}{\partial x^2}\Lambda_h(x,t;\omega)+2\alpha\frac{\partial}{\partial x}\Lambda_h(x,t;\omega)+\frac{e^{-\alpha x}}{\beta\overline{K}}e^{i\omega t}. \quad (39)$$

The solution of Eq. (39) with conditions Eq. (23) is

$$\Lambda_h(x,t;\omega)=\frac{2}{S_s\beta}\sum_{n=1}^{n=\infty}\frac{1-\cos(n\pi)}{n\pi}\exp(-\mu\frac{x}{L})\sin(n\pi\frac{x}{L})\frac{\exp(i\Omega_t)-\exp(-\theta_n t)}{\theta_n+i\omega}, \quad (40)$$

so that

$$\Lambda_q(t;\omega)=-2\frac{\overline{K}}{S_s L}\sum_{n=1}^{n=\infty}\frac{1-\cos(n\pi)}{n\pi}[n\pi\cos(n\pi\Upsilon)-\mu\sin(n\pi\Upsilon)]\frac{\exp(i\Omega_t)-\exp(-\theta_n t)}{\theta_n+i\omega}. \quad (41)$$

and thus

$$\left|\Lambda_q(t;\omega)\right|^2=4L^2\vartheta^2\sum_{n=1}^{n=\infty}\sum_{m=1}^{m=\infty}\frac{\Phi(m)\Phi(n)}{(\theta_n^2\tau_0^2+\Gamma^2)(\theta_m^2\tau_0^2+\Gamma^2)}\left[(\theta_m\theta_n\tau_0^2+\Gamma^2)(1+\Delta_1-\cos(\Omega_t)\Delta_2)-\Gamma\sin(\Omega_t)(\theta_m-\theta_n)\tau_0\Delta_3\right]$$

,

(42)

where

$$\Phi(y)=\frac{1-\cos(y\pi)}{y\pi}[y\pi\cos(y\pi\Upsilon)-\mu\sin(y\pi\Upsilon)], \quad (43)$$

Δ_1 = exp[-(θ_m+θ_n)t], Δ_2 = exp(-$\theta_m t$)+exp(-$\theta_n t$), and Δ_3 = exp(-$\theta_m t$)-exp(-$\theta_n t$).

At large times, Eq. (35) approach a finite value as

$$S_{rr}(\omega)=4\sum_{n=1}^{n=\infty}\sum_{m=1}^{m=\infty}\frac{1-\cos(m\pi)}{m\pi}\frac{1-\cos(n\pi)}{n\pi}\sin(m\frac{\pi}{2})\sin(n\frac{\pi}{2})\frac{\Theta_m\Theta_n+\Gamma^2}{(\Theta_m^2+\Gamma^2)(\Theta_n^2+\Gamma^2)}S_{\xi\xi}(\omega). \quad (44)$$

and the corresponding rainfall process is stationary. Combining Eq. (42) with Eq. (44) gives

$$\frac{S_{qq}(\omega)}{S_{\xi\xi}(\omega)}=16L^2\vartheta^2\left\{\sum_{n=1}^{n=\infty}\sum_{m=1}^{m=\infty}\frac{\Phi(m)\Phi(n)}{(\theta_n^2\tau_0^2+\Gamma^2)(\theta_m^2\tau_0^2+\Gamma^2)}\left[(\theta_m\theta_n\tau_0^2+\Gamma^2)(1+\Delta_1-\cos(\Omega_t)\Delta_2)-\Gamma\sin(\Omega_t)(\theta_m-\theta_n)\tau_0\Delta_3\right]\right\}$$

$$\times\left[\sum_{n=1}^{n=\infty}\sum_{m=1}^{m=\infty}\frac{1-\cos(m\pi)}{m\pi}\frac{1-\cos(n\pi)}{n\pi}\sin(m\frac{\pi}{2})\sin(n\frac{\pi}{2})\frac{\Theta_m\Theta_n+\Gamma^2}{(\Theta_m^2+\Gamma^2)(\Theta_n^2+\Gamma^2)}\right]. \tag{45}$$

Note that the nonstationarity in the hydraulic head or integrated discharge is introduced by a nonuniform thickness of the confined aquifer, even if the recharge field is stationary. Nonuniformity in the mean flow, for example, can also cause the nonstationarity in the statistics of random flow fields in heterogeneous aquifers (e.g., Rubin and Bellin, 1994; Ni and Li, 2006; Ni et al., 2010).

5 Conclusions

An analytical transfer function is developed to describe the spectral response characteristics of confined aquifers with variable thickness to the variation of the rainfall field, where the aquifer is directly recharged by rainfall at the outcrop of the aquifer. The rainfall-discharge process is treated as nonstationary in time, as it reflects the stochastic nature of the hydrological process. Any varying rainfall input at any time resolution can be convolved with the transfer function (or impulse response function) to simulate any discharge output of a linear model. The transfer function derived here, which relates the nonstationary spectra of the rainfall fluctuations to those of integrated discharge variation, has the potential to analyze the influence of

https://doi.org/10.5194/hess-2020-572
Preprint. Discussion started: 23 November 2020

Hydrology and Earth System Sciences
Open Access
Discussions

climate change on groundwater recharge variability.

The closed-form results of this work are developed on the basis of the Fourier-Stieltjes representation approach, which allows to analyze the effects of the controlling parameters in the models on the transfer function of the integrated discharge. It is founded that the persistence of rainfall fluctuations is greater for a smaller value of the characteristic time or length scale of the rainfall field, which in turn leads to greater variability of the integrated discharge field. The attenuating characteristic of the confined aquifer flow system is observed in the spectral domain. The variability of the integrated discharge in confined aquifer with variable thickness is increased with the thickness parameter α. The larger the aquifer diffusivity, the greater the spectrum (variability) of the integrated discharge.

Appendix A: Evaluation of Λ_h in Eq. (20)

The boundary-value problem describing the depth-averaged head fluctuations induced by the variation of recharge rate in frequency domain is given by Eqs. (22) and (23). Using the transformation,

$$\Lambda_h(x,t;\omega) = \exp[-\alpha(x+\frac{\alpha\overline{K}}{S_s}t)]U(x,t;\omega)\,, \tag{A1}$$

Eq. (22) in $\Lambda_h(x,t;\omega)$ together with Eq. (23) can be converted into a new (easier) one

https://doi.org/10.5194/hess-2020-572
Preprint. Discussion started: 23 November 2020

Hydrology and Earth System Sciences
Discussions

in a new variable $U(x,t;\omega)$ as

$$\frac{\partial}{\partial t}U(x,t;\omega)=\frac{\overline{K}}{S_s}\frac{\partial^2}{\partial x^2}U(x,t;\omega)+\frac{1}{\beta S_s}\exp(\frac{\overline{K}\alpha^2}{S_s}t)\Lambda_r(t;\omega)\,, \tag{A2}$$

with

$$U(x,0;\omega)=0\,, \tag{A3a}$$

$$U(0,t;\omega)=0\,, \tag{A3b}$$

$$U(L,t;\omega)=0\,. \tag{A3c}$$

The solution of Eqs. (A2) and (A3) can be found by the technique of separation of variables (e.g., Farlow, 1993) as

$$U(x,t;\omega)=\frac{2}{S_s\beta}\sum_{n=1}^{n=\infty}\frac{1-\cos(n\pi)}{n\pi}\sin(n\pi\frac{x}{L})\int_0^t\exp[-\upsilon_n(t-\tau)]\exp(\frac{\overline{K}}{S_s}\alpha^2\tau)\Lambda_r(\tau;\omega)d\tau\,, \tag{A4}$$

where $\upsilon_n=\overline{K}n^2\pi^2/(S_sL^2)$. With reference to Eq. (A1), the solution of Eqs. (22) and (23) is then given by Eq. (24).

Appendix B: Evaluation of Λ_ρ in Eq. (31)

Making use of the transformation,

$$\Lambda_\rho(x,t;\omega)=\exp(-\frac{t}{\tau_0})u(x,t;\omega)\,, \tag{B1}$$

leads Eqs. (31) and (32) to

$$\frac{\partial}{\partial t}u(x,t;\omega)=\frac{\lambda_0^2}{\tau_0}\frac{\partial^2}{\partial x^2}u(x,t;\omega)+\frac{1}{\tau_0}\exp[(\frac{1}{\tau_0}+i\omega)t]\,, \tag{B2}$$

with

https://doi.org/10.5194/hess-2020-572
Preprint. Discussion started: 23 November 2020

$$u(x,0;\omega)=0\,, \tag{B3a}$$

$$u(-\ell,t;\omega)=0\,, \tag{B3b}$$

$$u(\ell,t;\omega)=0\,. \tag{B3c}$$

In a similar way, based on the technique of separation of variables, Eqs. (B2) and (B3) arrive at the solution in the form

$$u(x,t;\omega)=2\sum_{m=1}^{m=\infty}\frac{1-\cos(m\pi)}{m\pi}\sin\left(m\pi\frac{x+\ell}{2\ell}\right)\frac{\exp[(1+i\Gamma)t/\tau_0]-\exp(-\varsigma_m t/\tau_0)}{\Theta_m+i\Gamma}\,, \tag{B4}$$

where $\varsigma_m = m^2\pi^2\eta^2$, $\eta = \lambda_0/(2\ell)$, $\Theta_m = 1+\varsigma_m$, and $\Gamma = \omega\tau_0$. The use of Eqs. (B1) and (B4) results in Eq. (33).

Data availability. No data was used for the research described in the article.

Author contributions. C-MC: Conceptualization, Methodology, Formal analysis, Writing - original draft preparation, Writing - review & editing.

C-FN: Conceptualization, Methodology, Formal analysis, Writing - original draft preparation, Writing - review & editing, Supervision, Funding acquisition.

W-CL: Conceptualization, Methodology, Formal analysis, Writing - original draft preparation, Writing - review & editing.

C-PL: Conceptualization, Methodology, Formal analysis, Writing - original draft preparation, Writing - review & editing.

I-HL: Conceptualization, Methodology, Formal analysis, Writing - original draft preparation, Writing - review & editing.

Competing interests. The authors declare that they have no conflict of interest.

Acknowledgements. Research leading to this paper has been partially supported by the grant from the Taiwan Ministry of Science and Technology under the grants MOST 108-2638-E-008-001-MY2, MOST 108-2625-M-008 -007, and MOST 107-2116-M-008 -003 -MY2.

References

Bear, J.: Hydraulics of groundwater, McGraw-Hill, New York, 1979.

Bear, J. and Cheng, A.H.-D.: Modeling groundwater flow and contaminant transport, Springer, Dordrecht, 2010.

Benoit, L., Vrac, M., and Mariethoz, G.: Nonstationary stochastic rain type generation: accounting for climate drivers, Hydrol. Earth Syst. Sci., 24(5), 2841-2854, 2020.

Christensen, N. S. and Lettenmaier, D. P.: A multimodel ensemble approach to assessment of climate change impacts on the hydrology and water resources of the Colorado River Basin, Hydrol. Earth Syst. Sci., 11(4), 1417-1434, 2007.

Cooper, H. H. and Rorabaugh, M.J.: Ground water movements and bank storage due to flood stages in surface streams, USGS Water Supply Paper 1536-J. Reston, Virginia: USGS, 1963.

https://doi.org/10.5194/hess-2020-572
Preprint. Discussion started: 23 November 2020

de Marsily, G.: Quantitative hydrogeology: Groundwater hydrology for engineers, Academic Press, Orlando, FL, 1986.

Eekhout, J. P. C., Hunink, J. E., Terink, W., and de Vente, J.: Why increased extreme precipitation under climate change negatively affects water security, Hydrol. Earth Syst. Sci., 22(11), 5935-5946, 2018.

Farlow, S. J.: Partial differential equations for scientists and engineers, Dover, New York, N. Y., 1993.

Gelhar, L. W.: Stochastic analysis of phreatic aquifer, Water Resour. Res., 10(3), 539-545, 1974.

Hantush, M.S.: Flow of ground water in sands of nonuniform thickness: 3. Flow to wells, J. Geophys. Res., 67(4), 1527-1534, 1962.

Long, A. J. and Mahler, B. J.: Prediction, time variance, and classification of hydraulic response to recharge in two karst aquifers, Hydrol. Earth Syst. Sci., 17(1), 281-294, 2013.

López, J. and Francés, F.: Non-stationary flood frequency analysis in continental Spanish rivers, using climate and reservoir indices as external covariates, Hydrol. Earth Syst. Sci., 17(8), 3189-3203, 2013

Lumley, J. L. and Panofsky, H. A.: The structure of atmospheric turbulence, John Wiley, New York, 1964.

https://doi.org/10.5194/hess-2020-572
Preprint. Discussion started: 23 November 2020

Hydrology and Earth System Sciences Discussions

Marino, M. A. and Luthin, J. N.: Seepage and Groundwater, Elsevier, New York, 1982.

Milly, P. C. D., Betancourt, J., Falkenmark, M., Hirsch, R. M., Kundzewicz, Z. W., Lettenmaier, D. P., and Stouffer, R. J.: Stationarity is Dead: Whither water management? Science, 319(5863), 573-574, 2008.

Molénat, J., Davy, P., Gascuel-Odoux, C., and Durand, P.: Study of three subsurface hydrological systems based on spectral and cross-spectral analysis of time series, J. of Hydrol., 222(1-4), 152-164, 1999.

Ni, C.-F. and Li, S.-G.: Modeling groundwater velocity uncertainty in nonstationary composite porous media, Adv. Water Resour., 29(12), 1866-1875, 2006.

Ni, C.-F., Li, S.-G., Liu, C.-J., and Hsu, S. M.: Efficient conceptual framework to quantify flow uncertainty in large-scale, highly nonstationary groundwater systems, J. Hydrol., 381(3-4), 297-307, 2010.

North, G. R., Shen, S. S. P., and Upson, R. B.: Sampling errors in rainfall estimates by multiple satellites, J. Appl. Meteor., 32(2), 399-410, 1993.

Olsthoorn, T.: Do a bit more with convolution, Groundwater, 46(1), 13-22, 2007.

Pedretti, D., Russian, A., Sanchez-Vila, X., and Dentz, M.: Scale dependence of the hydraulic properties of a fractured aquifer estimated using transfer functions, Water Resour. Res., 52(7), 5008-5024, 2016.

Pendergrass, A. G. and Hartmann, D. L.: Changes in the distribution of rain frequency and intensity in response to global warming, J. Clim., 27(22), 8372-8383, 2014.

Priestley, M. B.: Evolutionary spectra and non-stationary processes, J. R. Stat. Soc. Ser. B., 27(2), 204-237, 1965.

Razavi, S., Elshorbagy, A., Wheater, H., and Sauchyn, D.: Toward understanding nonstationarity in climate and hydrology through tree ring proxy records, Water Resour. Res., 51(3), 1813-1830, 2015.

Rinaldo, A. and Marani, A.: Basin scale model of solute transport, Water Resour. Res., 23(11), 2107-2118, 1987.

Rubin, Y. and Bellin, A.: The effects of recharge on flow nonuniformity and macrodispersion, Water Resour. Res., 30(4), 939-948, 1994.

Rugh, W. J.: Nonlinear system theory: the Volterra/Wiener approach, Johns Hopkins University Press, Baltimore, 1981.

Sang, Y.-F., Sun, F., Singh, V. P., Xie, P., and Sun, J.: A discrete wavelet spectrum approach for identifying non-monotonic trends in hydroclimate data, Hydrol. Earth Syst. Sci., 22(1), 757-766, 2018.

Trenberth, K.: Changes in precipitation with climate change, Clim. Res., 47(1), 123-138, 2011.

https://doi.org/10.5194/hess-2020-572
Preprint. Discussion started: 23 November 2020

Hydrology and Earth System Sciences
Open Access
Discussions

Figure captions

Figure 1. Graphical representation of the transfer function of the rainfall processes in Eq. (35) characterized by the time scale for different length scales, where the series calculation is truncated up to $M = N = 100$.

Figure 2. Influence of the thickness of the confined aquifer on the transfer function of the discharge flux, where the series calculation is truncated up to $M = N = 100$.

Figure 3. Influence of the aquifer diffusivity on the transfer function of the discharge flux, where the series calculation is truncated up to $M = N = 100$.